NASA

Technical Memorandum 85043

THE DRAG COEFFICIENT OF CYLINDRICAL SPACECRAFT IN ORBIT AT ALTITUDES GREATER THAN 150 km

F. A. Herrero

MAY 1983

National Aeronautics and
Space Administration

Goddard Space Flight Center
Greenbelt, Maryland 20771

THE DRAG COEFFICIENT OF CYLINDRICAL SPACECRAFT IN ORBIT AT ALTITUDES GREATER THAN 150 KM

A Report to the GRM Study Committee

F. A. Herrero*

Laboratory for Planetary Atmospheres

Goddard Space Flight Center

Greenbelt, Maryland 20771

May 1983

*Senior NAS/NRC Resident Research Associate

ABSTRACT

The spacecraft of the Geopotential Research Mission (GRM) are cylindrical in form and designed to fly with their longitudinal axes parallel to their direction of flight. The ratio of length to diameter of these spacecraft is roughly equal to 5.0. Other spacecraft previously flown had corresponding ratios roughly equal to 1.0, and therefore the drag produced by impacts on the lateral surfaces of those spacecraft was not as large as it will be on the GRM spacecraft. Since the drag coefficient is essentially the drag force divided by the frontal area in flight, lateral impacts, when taken into account make the GRM drag coefficient significantly larger than the coefficients used before for shorter spacecraft. A simple formula is derived for the drag coefficient of a cylindrical body flying with its long axis along the direction of flight, and it is used to estimate the drag for the GRM. The formula shows that the drag due to lateral surface impacts depends on the ratio of length-to-diameter and on a coefficient C_{LS} (lateral surface impact coefficient) which can be determined from previous cylindrical spacecraft flown with the same attitude, or can be obtained from laboratory measurements of momentum accommodation coefficients. In this report C_{LS} is obtained from flight data, and then used to estimate the accommodation coefficient at the large angles of incidence that occur on the lateral surface. On this basis, the GRM drag coefficient, without solar panels, is computed to be between 2.7 and 2.9 using a nose cone of half-angle of about 12°. Laboratory measurements at large angles of incidence are difficult to make with present techniques, and therefore are scarce or not reliable. The results show that previous extrapolations using accommodation coefficients measured at angles of incidence less than 65° are in error, and if used to compute the drag coefficient, would result in overestimates by 30% or more.

TABLE OF CONTENTS

LIST OF FIGURES

PREFACE

This report is the result of a review of the scientific literature on drag coefficients for spacecraft flying above 150 km altitude. The principal reason for the review was the large uncertainty in the estimate of the drag coefficient for the Geopotential Research Mission (GRM) spacecraft.

Considering the large body of data on drag estimates of previous missions it came as a surprise to see that there was large uncertainty in the magnitude of the drag coefficient for this mission. However, it soon became clear that most spacecraft that have been flown in the past either were not shaped like the GRM (long cylinders), or if cylindrical in shape, were tumbling in the decaying part of the orbit and appeared spherical on the average for the determination of their drag coefficients. Apparently the GRM spacecraft are among a very small number of spacecraft with long cylindrical form that are required to fly at critically low altitudes with guidance control to maintain minimum drag attitude.

Laboratory data on the applicable momentum accommodation coefficients have been surveyed, and measurements of the drag coefficient of one previous cylindrical spacecraft have been found in which attitude was controlled. This has been done with a view to converge upon a reasonable estimate of the drag coefficient for the GRM mission.

The study shows that extrapolations of laboratory data to obtain the momentum accommodation coefficient at large angles of incidence may be in error by a significant amount. Additional laboratory measurements of atom-to-surface momentum transfer are needed to understand this problem, and to fill the data gap that exists now at large angles of incidence. Perhaps experiments of a different nature from previous ones may be necessary in order to obtain reliable information in the large angle region. Previous experiments have relied on the sensitivity of the microbalance in order to detect the momentum transferred to the surfaces by atomic or molecular beams of

sufficiently high intensities. The molecular beams are produced by neutralization of an ion beam at the selected energy. Spacecraft velocities are of the order of 8 km/s and the relative kinetic energies of the atmospheric species (H, He, N_2, O, Ar, . . .) range from about 0.3 to about 15 eV. The most important energies for drag above 150 km correspond to atomic oxygen, 5.3 eV, and N_2, 9.4 eV. At those energies it is very difficult to obtain sufficiently high intensities from most ion sources, and the accuracy of the experiments is then limited by the sensitivity of the micro-balance. Standard methods using ion energy loss spectrometers could provide the required sensitivity and the capability for large angle measurements.

The concern expressed by Tom Keating, Study Manager of the GRM has been the driving force behind this study, and happily, we have found that there is sufficient data available to make a realistic estimate of the drag coefficient. I would like to acknowledge many helpful discussions with J. C. Ray of the APL/JHU, and in particular, his contribution of a copy of the report by A. Robertson. In the process we have also found a new method to compute the drag on the lateral surfaces of spacecraft.

F. A. Herrero

May 5, 1983

I. INTRODUCTION

The spacecraft proposed for the Geopotential Research Mission (GRM) are cylindrical in shape with a length-to-diameter ratio approximately equal to 5.0. It is a mission requirement that the spacecraft must fly at an altitude of 160 km for a minimum of 6 months beginning April 1989. Both spacecraft will be fueled and propelled by hydrazine thrustors which will fire continually in order to follow a drag-free orbit. Obviously, a minimum drag attitude should be maintained in flight to optimize fuel usage. Details on thrustor operation to follow a drag-free orbit and on attitude control for the GRM are given in a report by J. C. Ray and R. E. Jenkins, 1981. In that report, they also present the details of their drag coefficient calculation in which proper account is taken of the drag developed by impacts on the side surface of the spacecraft. The magnitude of the drag coefficient is critical to the GRM because of fuel limitations using the size of collapsible fuel tanks which are provided with current technology. The concern over its magnitude has arisen because the drag coefficient values that have been obtained from past spacecraft orbit decays suggest a value between 2.0 and 2.3. On the other hand, rigorous calculations (Ray and Jenkins, 1981; Fredo and Kaplan, 1980) that use commonly accepted values for the momentum accommodation coefficients (Knechtel and Pitts, 1971) suggest a value of about 4.0 or higher for the bare cylindrical body of the GRM.

In this report, the main question addressed is that of the magnitude of the drag coefficient of a cylindrical body, with a length to diameter ratio of about 5.0, and flying with its long axis approximately parallel to the direction of flight.

The drag force on a body moving through the air is defined as that component of force produced by the air in a direction opposite the direction of flight. The drag coefficient is given by the relation

$$C_D = \frac{F_D}{\frac{1}{2} \rho V^2 A_r} \quad . \tag{1}$$

where F_D is the drag force, ρ the density of the surrounding air, and V the velocity of the body. The area A_r is a reference area that must equal the area projected by the body along the direction of flight. Care must be taken in defining this reference area to ensure that all computations of the drag coefficient are consistent. However, it must be recognized that the side surfaces of the spacecraft contribute drag in addition to the drag due to the projected area A_r. So, it is not surprising that the drag coefficient increases with the length of the spacecraft.

The next period of maximum solar activity occurs in 1991. If put into orbit in 1989, the GRM spacecraft will be flying during the onset of solar maximum, and may encounter very high atmospheric densities and correspondingly high drag forces. The drag coefficient must be known within certain bounds together with the atmospheric density in order to predict the expected lifetime of the mission with high reliability. In this report we obtain upper and lower bounds on the drag coefficient of the bare GRM cylinders to be used in orbit lifetime calculations using upper and lower bounds on the expected densities.

The next section reviews some of the basic notions which would apply at altitudes of 150 km or more regarding drag forces. This is done mainly in order to point out the role played by the accommodation coefficient and the importance of the lateral surface in the drag coefficient. In the third section an expression is derived which gives the drag coefficient explicitly in terms of the diameter-to-length ratio, and it is used in the fourth section to compute the GRM cylinder drag coefficient using only previous flight data which give the drag coefficient of a cylindrical spacecraft flown with attitude control. The fifth section is not essential to this report and represents work in progress. However, it is included to demonstrate a method of obtaining the accommodation coefficient at large angles of incidence from flight data. In this regard, the GRM will offer a unique opportunity to measure the drag and accommodation coefficients in flight with accuracies not achieved before if the density, temperature and composition are measured in-situ with a small sensor similar to those flown before (Spencer et al., 1973). The last section gives the conclusions and recommendations.

II. DRAG FORCE IN A RAREFIED ATMOSPHERE

In this section we review the basic theory of the drag force on a body moving with high velocity in a rarefied atmosphere. We show that the drag above 150 km is due to individual impacts on the surface of the spacecraft, and describe the basic parameters that are generally used to compute the drag force.

The Knudsen Number

We can say that a spacecraft flies in a rarefied gas if the mean free path of the molecules in the gas, λ, (average distance between collisions) is much larger than the linear dimensions of the spacecraft. The parameter commonly used to give the degree of rarefaction in a gas is the Knudsen number defined by

$$K = \frac{\lambda}{L}, \tag{2}$$

where, for our purposes, L is some average linear dimension of the spacecraft. When $K \gg 1$, we can be sure that molecules re-emitted from the spacecraft surface will not impact other gas molecules until very far away from the spacecraft. So, under conditions of very high Knudsen number, the free stream velocity distribution of the gas near (in front of and to the sides) the spacecraft is not altered by the re-emitted molecules. Therefore, the velocity distribution of the free gas stream is Maxwellian with a bulk velocity equal to the negative of the spacecraft velocity. That is,

$$f(\vec{v}) = n\left(\frac{1}{\pi a^2}\right)^{3/2} e^{-[(v_x - V)^2 + v_y^2 + v_z^2]/a^2} \tag{3}$$

Here we have chosen the spacecraft velocity to be in the negative direction to the x-axis with magnitude V, as shown in Figure 1a for a coordinate frame at rest in the gas. $a = (2kT/m)^{1/2}$ is the most probable speed of the molecules of the gas. The velocity distribution of eq (3) is specified in the spacecraft coordinates (shown in Figure 1b), and there $V > 0$.

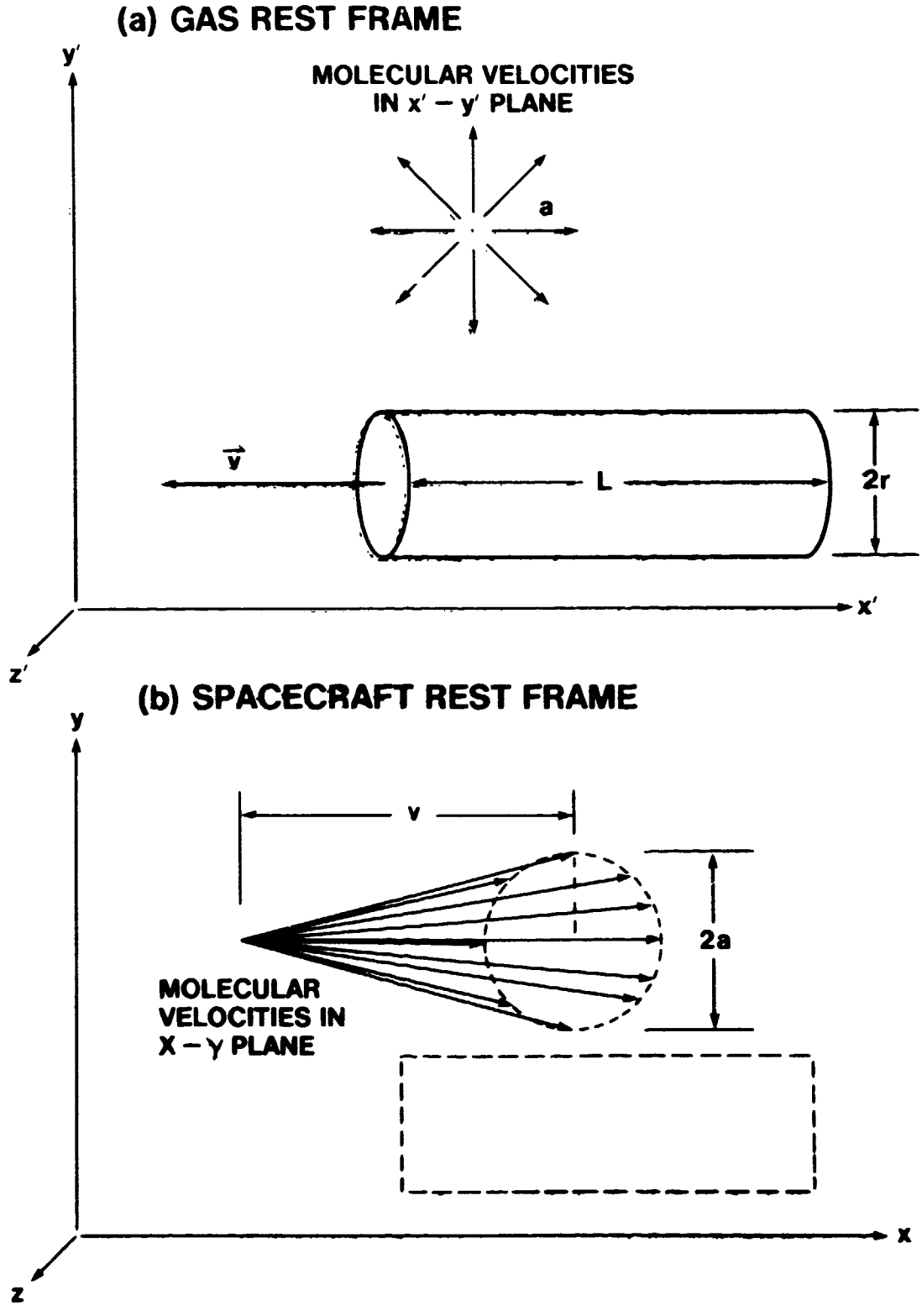

Figure 1. Distribution of molecular velocities in two coordinate systems.

The molecular rays shown in Figure 1a, the gas rest frame, have lengths equal to the most probable speed a, and they are randomly oriented. In Figure 1b, the spacecraft rest frame, the molecular rays have lengths roughly equal to V, but we see that they are dispersed in direction and magnitude by the thermal motion, represented by the width 2a. Both parts of the figure show that, from any point in space above, below or to the sides of the spacecraft, as many molecules move toward the spacecraft as move away from it. In other words, of all the molecules that have sufficient speed to reach the sides of the spacecraft from any point in space, only one half of those will reach it, the other half moving in the opposite direction.

Likely values of K may be obtained from a knowledge of the air density and the average collision cross sections at the altitudes and temperatures of interest. The mean free path is inversely proportional to the number density n, in particles/unit volume, and to the collision cross section σ, in units of area. It is given by (Loeb, 1961)

$$\lambda = \frac{1}{\sqrt{2}} \frac{1}{n\sigma} \quad . \tag{4}$$

and it is tabulated in the 1976 U. S. Standard Atmosphere as a function of altitude. Figure 2 gives the mean free path in the altitude range of interest here. For the GRM, the Knudsen number is numerically equal to the mean free path since the GRM spacecraft diameter is roughly 1.0 meter.

When K is less than about 40, as it may happen at 150 km under extreme solar active conditions, it is possible that the re-emitted molecules may undergo their first collision sufficiently close to the spacecraft to begin to modify the incident stream in front and to the sides of the spacecraft. Under these conditions, the re-emitted molecules partially shield the surface of the spacecraft from direct impact by molecules in the free stream. Some reduction in drag may result. This effect may be of some importance at 150 km because the thermal velocity of the re-emitted molecules is about one-tenth of the free stream velocity. For further details on this effect, see G. E. Cook (1965) and references cited therein.

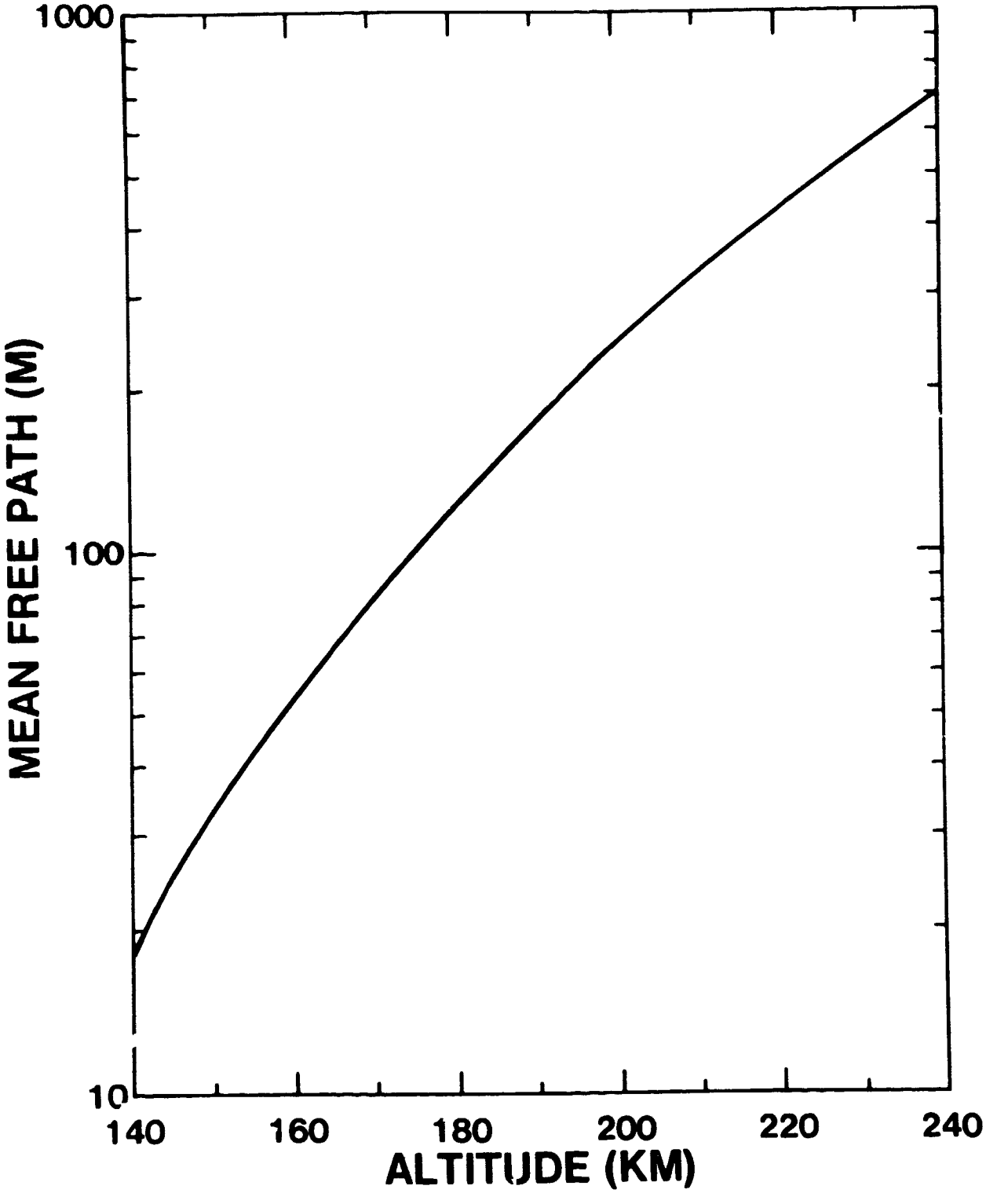

Figure 2. Mean free path in the atmosphere as a function of altitude.

The Drag Force

We begin with a discussion of the drag force on a simple surface. Consider a flat square surface A of side ℓ moving through a rarefied gas with velocity V, and having its normal vector oriented at an angle θ with V (angle of attack) as shown in Figure 3. We assume that the gas is at rest so that the line of impact of the gas molecules with the surface is parallel with the line of flight. A bulk velocity in the gas (e.g., a wind) will have the effect of changing the angle θ, and must be taken into account when measured. For the remainder, we assume that there is no bulk velocity in the gas rest frame. If the Knudsen number λ/ℓ is much larger than 1.0, then the total force on the surface may be expected to arise entirely from the sum of the forces exerted by the individual free stream molecules. Keeping in mind that the drag force is that component of force along the line of impact, we compute the net momentum delivered to the surface per unit time along that line by a stream of molecules impacting at an angle of incidence given by θ. If p_i is the momentum of the incident molecules, and p_r the momentum carried away by the reflected or re-emitted molecules along the direction of flight, the net momentum delivered along this direction is

$$p_D = p_i + p_r . \tag{4}$$

It is understood that the incident momentum p_i is positive when directed toward the surface, whereas the reflected momentum is positive when directed away from the surface. It is possible to compute p_i for a Maxwellian gas described by eq (3), but p_r depends on surface condition and on the specific molecule-surface interaction potential. If the surface condition were known and stable, then, in principle, the interaction potential could be computed, and with it a reliable value for p_r could be obtained. For example, experimental results show (Thomas, 1980) that the nature of adsorbed layers may be very important in atom-surface interaction. It has been observed that atoms linger on, or accommodate most easily when incident upon a surface covered with atoms of the same species than when incident on a clean surface covered with atoms of a different species, and

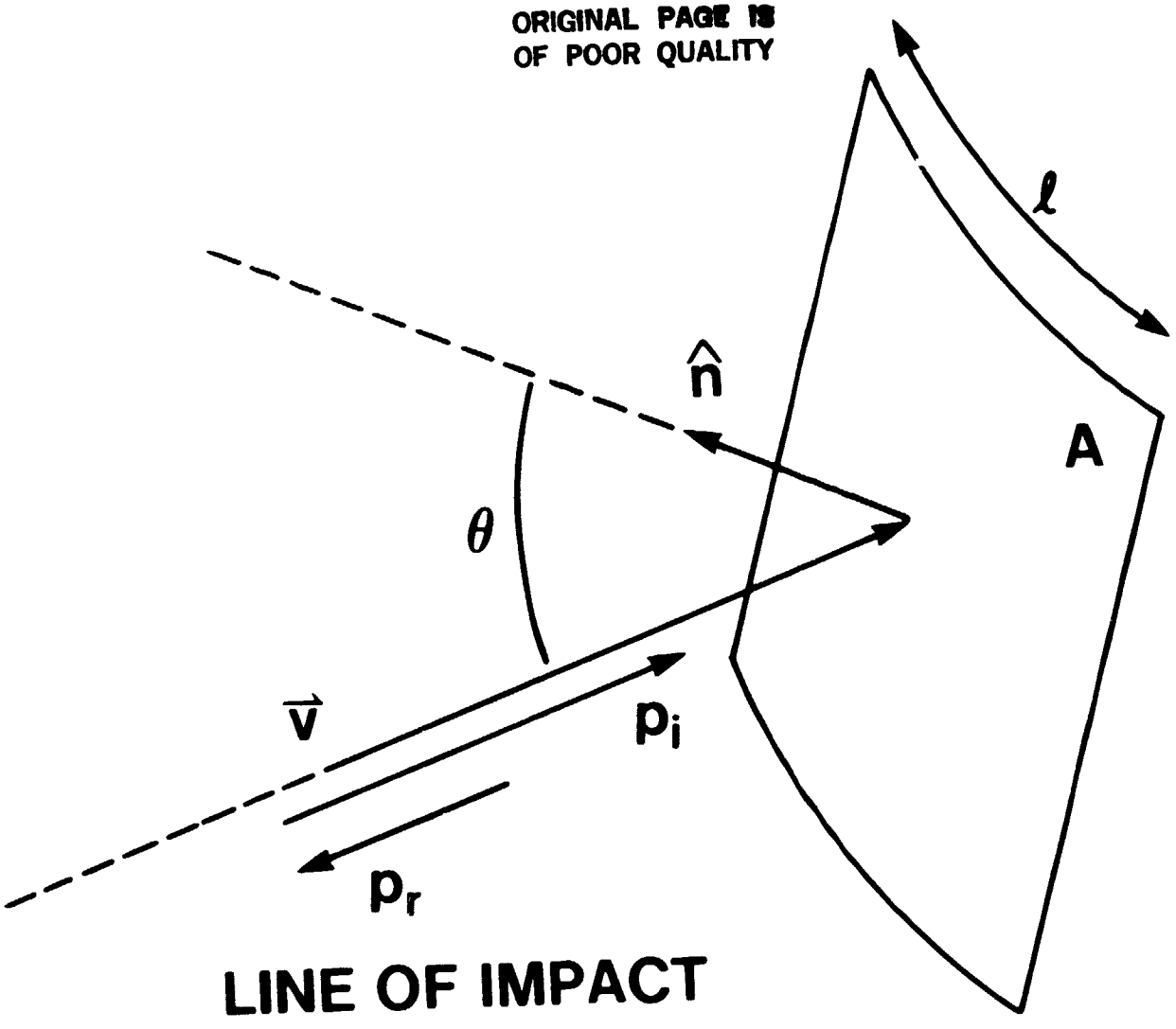

Figure 3. Molecular momentum $\vec{p}_i$ is incident on a surface element at angle θ with the surface normal. $\vec{p}_r$ is the component of reflected or re-emitted momentum along the line of $\vec{p}_i$, labelled the line of impact.

and this may be due to resonant exchange between identical particles, or to the optimum momentum transfer that takes place between two equal masses. We note that the density at 160 km is such that a monolayer of N_2 or 0 would be deposited in several seconds (Cook, 1965). So, one would expect that the impacting atoms and molecules should accommodate readily to spacecraft surfaces, and perhaps predictable results may be obtained with surfaces of minimum roughness.

The idea of accommodation is closely related to the time spent by the molecule "lingering" on the surface and to the notion of diffuse reflection (Loeb, 1961). Diffuse reflection means

that the molecules are re-emitted randomly from the surface, and this must mean that all correlation with the incident momentum vector has been lost. It is difficult to think that all correlation could be lost in a single collision, so we are led to conclude that the notion of diffuse reflection means that the molecule has suffered several collisions on the surface before being re-emitted. That is, the molecule has "lingered" on the surface for several collision times.

At the other extreme, we have the situation of a single elastic collision before re-emission. This leads to the notion of specular reflection. We may think that at high velocity impacts an incident molecule is less likely to linger because the time spent moving toward the surface is short, and the effects of the interaction potential are not felt until very close to one of the surface atoms. If this were true, we would conclude that specular reflection should be important only for velocities higher than some value. For velocities near that value, we might expect a gradual transition from diffuse to specular until such a high velocity is reached that channeling occurs and effective penetration of the surface occurs. The general picture we have just described is consistent with experimental results (e.g., O'keefe and French, 1969; Jakus and Hurlbut, 1969; Smith and Saltsburg, 1966; Devienne et al., 1966). However, the precise behavior at the velocities of interest here is still somewhat nebulous.

Returning to equation (4) above, we can write the momentum transferred along the direction of θ when the re-emitted molecules are fully accommodated to the surface as

$$p_{acc} = p_i + p_s \,, \tag{5}$$

where p_s is the average momentum carried away in the direction of θ by molecules that fully accommodate to the surface temperature T_s. We turn now to the definition and discussion of the momentum accommodation coefficients.

Momentum Accommodation Coefficients

A gas that fully accommodates to a surface interacts in such a way that after colliding with the surface, the distribution function of the re-emitted gas corresponds exactly to the surface temperature. Thus, the term 'accommodation' is significant in a statistical sense. The term is applied to accommodation in energy and momentum, and the usefulness of the definition stems only from the fact that measurable parameters can be derived from it. We can see that it is possible to measure the degree of accommodation if we took the ratio of equations (4) and (5). For 100% accommodation, we must have the condition

$$p_{net} = p_{acc} \cdot$$

So, we can define an accommodation coefficient to specify the degree of momentum accommodation with a surface by

$$\alpha(\theta) = \frac{p_i - p_r}{p_i - p_s} , \tag{6}$$

where we show the coefficient as a function of θ to indicate that it depends on direction, and is basically a vector quantity. In this definition we have taken the differences between the momentum components so that $\alpha(\theta) < 1$ when the degree of accommodation is less than 100%.

Conventionally, the momentum accommodation coefficient is specified by two components, the normal and the tangential (Schaaf and Chambre, 1958). The normal, or perpendicular momentum accommodation coefficient is given by

$$\alpha_n = \frac{p_{ni} - p_{nr}}{p_{ni} - p_s} \tag{7}$$

and the tangential by

$$\alpha_\tau = \frac{p_{\tau i} - p_{\tau r}}{p_{\tau i}} \quad , \tag{8}$$

where the subscripts n and τ stand for normal and tangential, respectively.

Notice that since p_s is always perpendicular to the surface, the subscript n has been suppressed. Of course, this follows because the velocity distribution of a Maxwellian gas emitted from the surface is isotropic, and for the same reason $p_{\tau s} = 0$, and does not appear in the denominator of eq (8).

Using the accommodation coefficients we can compute the drag force on any surface as a function of the angle of attack. The net pressure on the surface is given by

$$\text{Pressure} = p_{ni} + p_{nr} = (2 - \alpha_n)\, p_{ni} + \alpha_n\, p_s \quad , \tag{9}$$

and the net shear comes from the difference

$$\text{Shear} = p_{\tau i} - p_{\tau r} = \alpha_\tau\, p_{\tau i} \quad . \tag{10}$$

The quantities p_{ni}, $p_{\tau i}$, and p_s are easily computed, and are given in numerous references in the literature (e.g., Schaaf and Chambre, 1958, H. S. Tsien, 1946). The quantities p_{nr} and $p_{\tau r}$ are usually measured in laboratory experiments as discussed in section V, or may be obtained from drag and lift coefficients measured in-flight.

Schaaf and Chambre (1958) have shown that the above coefficients can be used to obtain the pressure p in terms of the normal momentum delivered (with α_n), and the shear stress (with α_τ). Using their results, we write

$$p = \frac{\rho}{2s^2}\left[\left((2 - \alpha_n) + \frac{\alpha_n}{2}\sqrt{\frac{\pi T_s}{T}}\right) g(s) + \frac{2 - \alpha_n}{2}\left(1 + \text{erf}\,(s)\right)\right] , \tag{11}$$

and

$$\tau = \frac{\alpha_\tau \rho V^2 \sin\theta}{2} \frac{g(s)}{s} \quad , \tag{12}$$

where

$$g(s) = \frac{s}{\sqrt{\pi}}(e^{-s^2} + s^2 (1 + \text{erf}(s))) \quad , \tag{13}$$

and

$$s = \frac{V}{a} \cos\theta \quad . \tag{14}$$

The drag force on a surface element dA moving with velocity V in a gas at rest may be computed with the aid of Figure 4.

From the figure,

$$d F_D = (p \cos\theta + \tau \sin\theta)\, dA \quad , \tag{15}$$

where p and τ are given by equations (11) and (12).

For zero angle of attack ($\theta = 0$),

$$d F_D = p dA \quad , \tag{16}$$

where p must be evaluated using eq (11) for s = V/a. For a 90° angle of attack,

$$d F_D = \tau dA \quad . \tag{17}$$

For this case, s = 0 and g(s) = 0. However, $g(s)/s = 1/\sqrt{\pi}$, and

$$d F_D = \frac{\alpha_\tau \rho V^2}{2\sqrt{\pi}} dA \quad . \tag{18}$$

Thus, the drag force on the sides of the cylinder may be obtained using equation (18). This requires knowledge of α_τ at 90° incidence angle. As we will see below, this number is not known from experimental data. The microscopic state of the surface will affect the value of α_τ for angles very close to 90°, so that if known for some laboratory surfaces, its magnitude would not be reliable for application to spacecraft. We will see in section V that previous extrapolations (Fredo and Kaplan, 1981) of the laboratory measurements of Knechtel and Pitts (1973) give $\alpha_\tau = 0.6$ at 90°, and that this value would lead to an overestimate in the drag in our computation below.

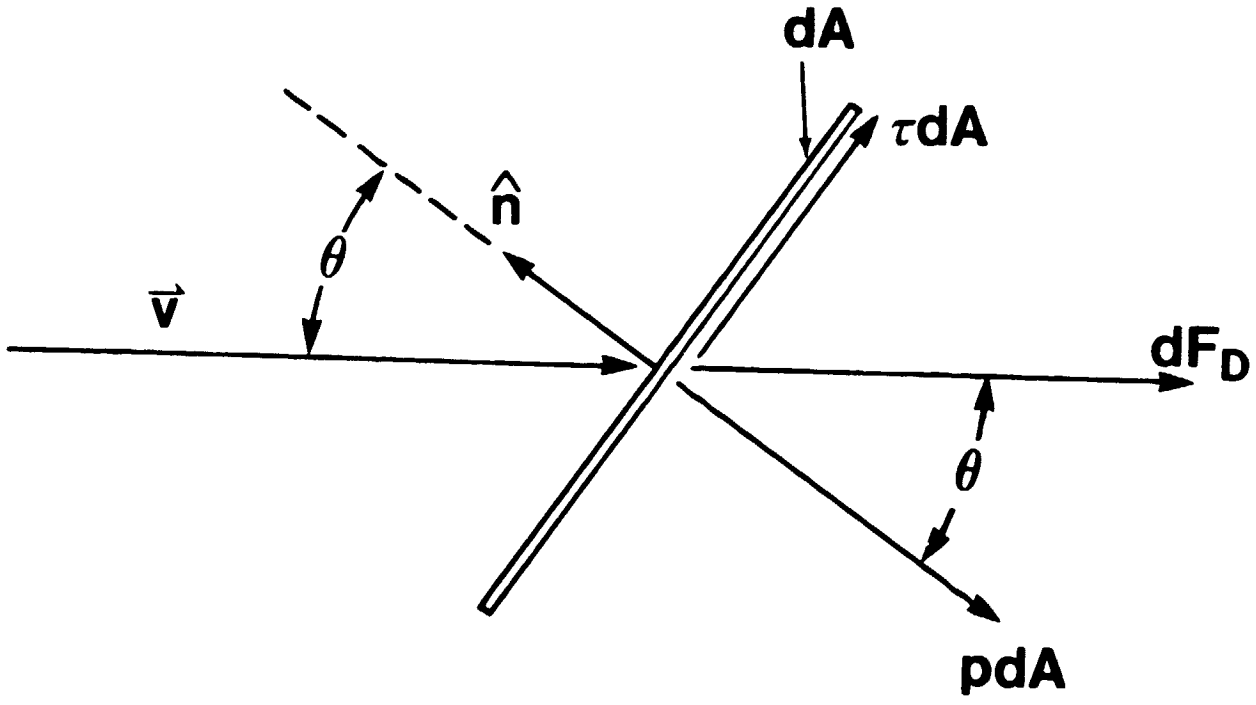

Figure 4. Molecules incident on surface dA from the left with velocity $\vec{v}$ exert a force dF_D which is the vector sum of the normal component pdA, and the tangential component τdA.

III. THE DRAG COEFFICIENT OF A CYLINDRICAL BODY

In the previous section we saw that it may be possible to use equations (11) and (12) to carry out a calculation of the drag coefficient, but that in order to take proper account of the lateral surface drag, the accommodation coefficient would have to be known for a 90° angle of incidence.

Now we pursue a description of the drag coefficient which will enable us to make direct use of previous flight data in a calculation of the drag including the effect of the lateral surfaces. This description depends on the fact that lateral surface impacts do not occur at 90° on the average, but rather at some average angle $\bar{\theta}_i$, close to but less than 90°, determined by the magnitude of the thermal motion, as discussed with Figure 1b. The resulting equation derived below (eq (32)) is general in terms of the coefficient C_{LS} for the lateral surface. The value obtained for C_{LS} below depends explicitly on the average angle of incidence $\bar{\theta}_i$. Nonetheless, we emphasize that our drag coefficient estimate does not require a knowledge of this angle at this point. The value of this angle depends on the specific form given to the momentum flux, and this represents work in progress at the moment. The relation of this work to the experimental work of Boring and Humphris, Knechtel and Pitts, and Seidl and Steinheil will be given in section V.

Referring back to Figure 1b, we see that as many molecules will be moving in the positive y-direction as in the negative y-direction. Therefore, no matter how fast the spacecraft moves, there will always be some molecules striking the sides and imparting some momentum there. Also, we see that of all the molecules above the spacecraft only those with negative v_y may reach the side. Similarly for the ones below, only those with positive v_y may contribute to the lateral surface drag. Now, the average velocity component in the x-direction is just V. The average upward (or downward) velocity will be smaller than V, and approximately equal to the most probable speed; we call it $\bar{v}$. Thus, the molecules will impact the lateral surface at an average angle of incidence given by

$$\bar{\theta}_i = \tan^{-1}\left(\frac{V}{\bar{v}}\right) . \qquad (19)$$

For our purposes, we take $\bar{v} = a$, and for the temperature, orbital velocity and composition at 160 km, we obtain $\bar{\theta}_i \simeq 84°$. The average incident velocity vector is

$$\vec{V}_i = \hat{i}\, V + \hat{j}\, \bar{v} \quad . \tag{20}$$

In the following we obtain an equation (eq (24)) for the drag force on a body moving through a gas with no thermal spread ($\bar{v} = 0$). Then we modify the result to take into account the thermal motion with eqs. (19) and (20).

The gas momentum flux density with respect to the spacecraft may be approximated for high velocities by the flux in the direction of V:

$$\vec{J}_p = \rho\, V\, \vec{V} \quad . \tag{21}$$

Consider the momentum delivered to an infinitesimal area element dA which moves through the gas such that its normal makes an angle θ with the velocity vector V as shown in Figure 4.

The net momentum delivered to dA is given by eq (4). So, the fraction of the incident momentum transferred to the surface is

$$f_n(\theta) = \frac{p_i + p_r}{p_i} = 1 + f(\theta) \quad . \tag{22}$$

where we have defined $f(\theta) = p_r/p_i$, the fraction of momentum reflected or re-emitted in the direction of p_i. The function $f(\theta)$ has been measured in the laboratory by Boring and Humphris (1973), and those measurements formed the basis for the initial approach taken in this computation.

Multiplying the incident momentum flux density, eq (21), by the area projected by dA gives the total momentum intercepted per unit time by dA. Subsequent multiplication by $f_n(\theta)$, eq (22), gives the force on dA in the direction of p_i. We get

$$d F_D = (1 + f(\theta)) \rho V^2 \cos\theta \, dA \quad . \tag{23}$$

The drag force on a body defined by surface Σ is then

$$F_D = \int_{\Sigma} (1 + f(\theta)) \rho V^2 \cos\theta \, dA \quad , \tag{24}$$

Where Σ is made up of those parts of the body surface whose normals have non-zero positive components in the direction of flight. Using the definition of the drag coefficient (eq. (1) above) gives

$$C_D = 2[1 + \frac{1}{A_r} \int_{\Sigma} f(\theta) \cos\theta \, dA] \quad . \tag{25}$$

For a flat plat plate at angle θ, the drag coefficient is

$$C_D = 2 [1 + f(\theta)] \quad . \tag{26}$$

This is precisely the relation used by Boring and Humphris (1973) to obtain the drag coefficient from their measurements of the ratio $f(\theta)$.

This formulation ignores the effect of the thermal motion of the gas on the side surfaces of a cylindrical spacecraft flying with its axis parallel to its velocity vector because we have neglected the thermal motion of the molecules in the beam. That is, those surfaces which point at 90° to V. Thus, equations (24) and (25) lead to serious error at surface angles of attack $\theta \geqslant 90°$. Equation (25) is very similar to the equation used by Moe and Tsang (1973) to study drag coefficients of cones and cylinders. Figure 3 of their paper shows that the cylinder drag is zero for zero angle of attack. However, we will show now that it is possible to use the experimental data obtained by Boring and Humphris in conjunction with eq (24) to compute the total drag on the spacecraft including the effect of the thermal motion on the side surfaces.

Figure 5a shows a cylindrical body of length L and radius r. For this example, we shall assume that the front face is a flat plate whose normal coincides with the cylinder's axis as shown in the figure. The area of the front face is designated A_f, and the drag coefficient associated with the front face C_{Df}. The total drag force on the cylindrical body is given by

$$F_D = \frac{1}{2}\rho\, V^2\, C_{Df}\, A_f + F_s \quad . \tag{27}$$

where F_s is the drag force exerted on the sides of the cylinder.

In order to obtain F_s we first compute the drag force on a thin strip on A_s, and then integrate over A_s. The drag component for each thin strip dA_s is obtained using eq. (23) above with reference to Figure 5b. The angle θ in this case is the average angle at which the gas molecules strike the sides. This angle is given by equation (19). The force along V_i on dA_s is

$$dF = \frac{1}{2}\rho\, V_i\, (1 + f(\theta))\cos\theta\, dA_s \quad . \tag{28}$$

where the factor ½ is indicative of the fact that only one half of the molecules given by the density ρ may reach the side surfaces. The component of this force that contributes to the drag on the cylinder is shown as dF_s in the figure, and is

$$dF_s = \sin\theta\, dF \quad . \tag{29}$$

Since θ is the same for all strips on the side surface, integration gives

$$F_s = \frac{1}{2}\rho\, V_i^2\, A_s \sin\theta\cos\theta\, (1 + f(\theta)) \quad . \tag{30}$$

Substituting (30) into (27), and using the areas $A_s = 2\pi rl$, and $A_f = \pi r^2$, the total drag force on the cylinder becomes

$$F_D = \frac{1}{2}\rho\, V^2\, A_f \left[C_{Df} + \frac{2L}{r}\cos\theta\, (1 + f(\theta))\right] \quad . \tag{31}$$

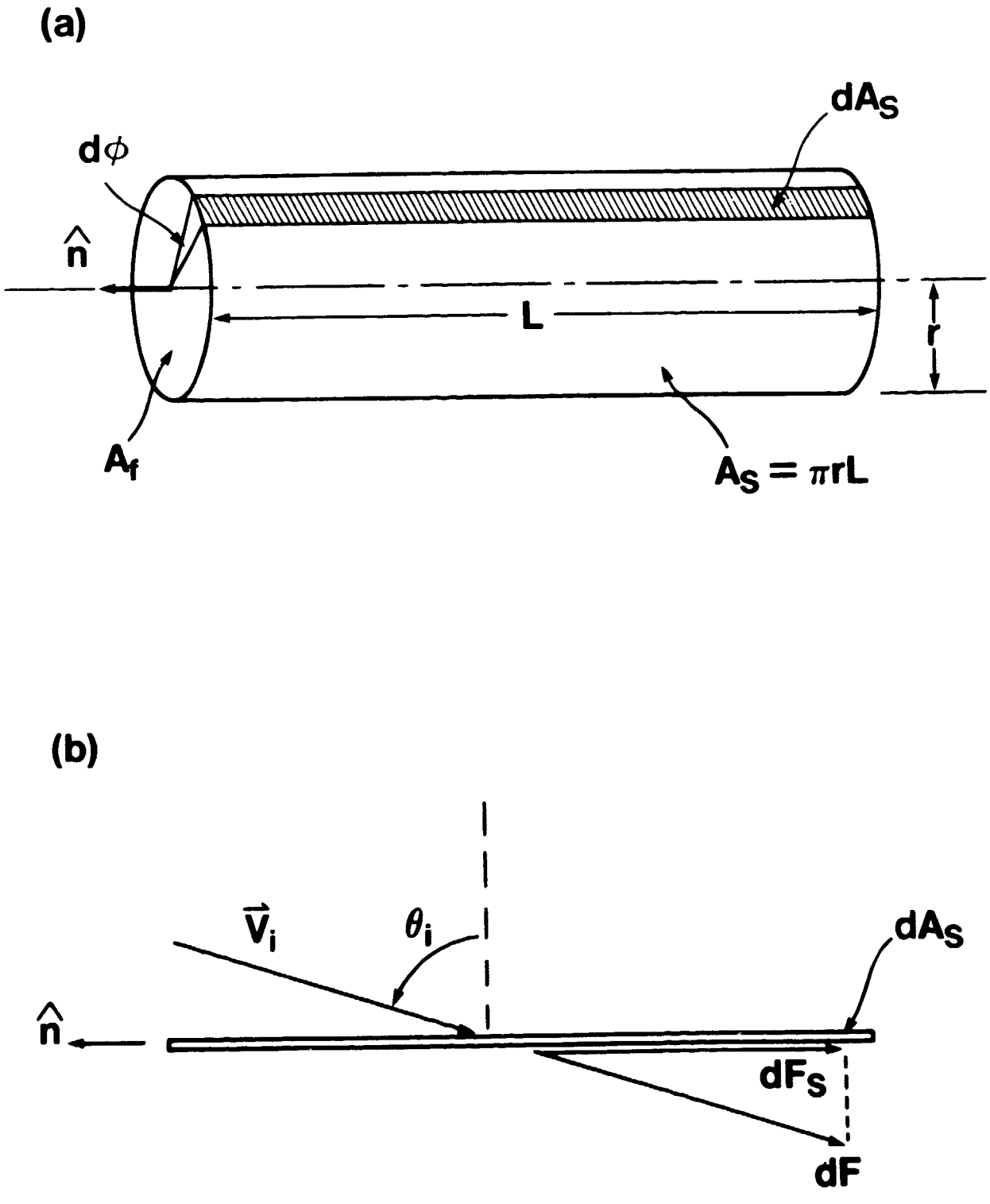

Figure 5. (a) Cylindrical geometry for lateral surface drag computation. (b) dF_s is the component of force contributing to the lateral surface drag. The component perpendicular to dA_s (not shown) is cancelled by an identical component from opposite side of the cylinder.

where we have eliminated V_i using eqs (19) and (20). From this, we obtain the drag coefficient for the cylinder

$$C_D = C_{Df} + \frac{2L}{r} C_{LS} \quad . \tag{32}$$

where we have defined the lateral surface coefficient as

$$C_{LS} = \cos\theta \; (1 + f(\theta)) \quad . \tag{33}$$

Equation (32) is perhaps an obvious result. Intuitively, we know that the drag due to the lateral surface must be directly proportional to the length of the cylinder. Equation (24) tells us that the length of the cylinder is to be specified in units of the radius of the cylinder, since the radius is the basic parameter for the frontal area. We note that the ratio of lateral area to frontal area is 2L/r, the factor that multiplies C_{LS}.

IV. DRAG COEFFICIENT ESTIMATE FOR GRM

In this section we present the drag coefficient measured for a cylindrical spacecraft flown with sufficient attitude control to maintain zero angle of attack. We use that drag coefficient with the dimensions of that spacecraft to obtain the value of the lateral surface coefficient C_{LS}, and then obtain the drag coefficient for the GRM.

Lateral Surface Coefficient Estimate

We refer to a report by A. Robertson (1971) in which the drag coefficient was measured for an Agena rocket that was put into orbit in the altitude range from 140 to more than 180 km. The spacecraft's form was cylindrical with a nose cone of about 12° half-angle with a base diameter of 1.5 meters. The base of the cone was continued by a cylinder of the same diameter with a length of about 11 meters, and finally a tail section 2.7 meters long. For angles of attack near zero, the tail section contributed very little to the drag because it was masked by the

cylinder section. So the drag coefficient consisted of contributions from the nose cone and the lateral surface of the main cylinder.

We compute the drag coefficient for the nose cone first. Applying equation (25) to a cone of half-angle $\phi = 12°$, we get

$$C_{Df} \simeq 1.5 \pm 0.1,$$

where we have used $A_{cone} = \pi r^2/\tan\phi$ and $f(78°) \simeq -0.25 \pm .05$ estimated from the data on Table I, section V. The lateral surface coefficient is found using Robertson's high and low values for C_D (Agena).

$$C_D \text{ (Agena-high)} = 3.6$$

$$C_D \text{ (Agena-low)} = 3.3$$

$$\frac{L}{r}\text{(Agena)} \simeq 15$$

$$\frac{L}{r}\text{(GRM)} = 10.0$$

Using these numbers and $C_{Df} = 1.5$ we get from eq (32)

$$C_{LS} \text{ (high)} = 0.07$$

$$C_{LS} \text{ (low)} = 0.06$$

The GRM upper and lower bounds follow from eq (32):

$$C_D \text{ GRM (high)} = 2.9$$

$$C_D \text{ GRM (low)} = 2.7 \quad .$$

V. COMPARISON WITH LABORATORY DATA

Measurements of momentum transfer parameters appropriate to this calculation have been found in the literature. They have been reported by Knechtel and Pitts (1973), Boring and Humphris (1973), and Seidl and Steinheil (1974). Unfortunately, the definitions of the parameters of interest are all different, and a brief description of each experiment is necessary in order to reduce all parameters to one common definition. The three experiments were very similar in their apparatus makeup. They used a molecular beam incident on a sample surface and measured the resultant force on the surface with a microbalance.

By far the most straightforward parameter definition was given by Boring and Humphris (1973). They were interested in determining drag coefficients only; therefore they measured the momentum components along the direction of the incident beam only. The microbalance was used to measure the momentum delivered to a sample surface whose plane could be oriented with respect to the axis of the incident molecular beam. They measured the incident momentum p_i and the reflected momentum p_r along the line of incidence for several orientation angles from 15° to 75°, and reported the ratio of these quantities as a function of the angle of incidence. Their results are given in the 8th column of table I below. The results of all three experiments are given in that Table. The first column gives the angle of incidence and the subsequent columns give α_n, α_τ and p_r/p_i for each experiment and for each angle. The following paragraphs describe the results of the other two experiments and the derivation of p_r/p_i to compare all three consistently.

Seidl and Steinheil carried out similar measurements with a microbalance, except that they made two measurements for each angle of incidence. Those two measurements were done 90° apart, and therefore could be used to separate the normal and tangential components of the momentum to obtain the accommodation coefficients. They preferred not to include the momentum of fully accommodated molecules issuing from the surface, so their normal accommodation

coefficient is different (and more tractable) from the standard definition of equations (7) and (8) above. Figure 6 shows the experimental configuration described by them, and their measurements are listed in columns 2 and 3 of Table I. We use the vector and angle diagrams in the figure to obtain the ratio p_r/p_i in order to make valid comparisons with the data of Boring and Humphris. They defined the momentum accommodation coefficients by

$$\text{(normal)} \quad \alpha_n = \frac{p_{ni} - p_{nr}}{p_{ni}} \quad , \tag{34}$$

and

$$\text{(tangential)} \quad \alpha_\tau = \frac{p_{\tau i} - p_{\tau r}}{p_{\tau i}} \quad , \tag{35}$$

From the figure, we can see that the ratio is

$$\frac{p_r}{p_i} = \frac{p_{nr}}{p_i} \cos\theta_i - \frac{p_{\tau r}}{p_i} \sin\theta_i \quad ,$$

but, using equations (34) and (35) the components p_{nr} and $p_{\tau r}$ are given by

$$p_{nr} = p_i \cos\theta_i (1 - \alpha_n) \quad ,$$

and

$$p_{\tau r} = p_i \sin\theta_i (1 - \alpha_\tau) \quad ,$$

so, the ratio is simply

$$\frac{p_r}{p_i} = (1 - \alpha_n) \cos^2\theta_i - (1 - \alpha_\tau) \sin^2\theta_i \quad , \tag{36}$$

Now we can obtain the ratio p_r/p_i using the values of α_n and α_τ of Seidl and Steinheil. These are tabulated in column 4 of Table I.

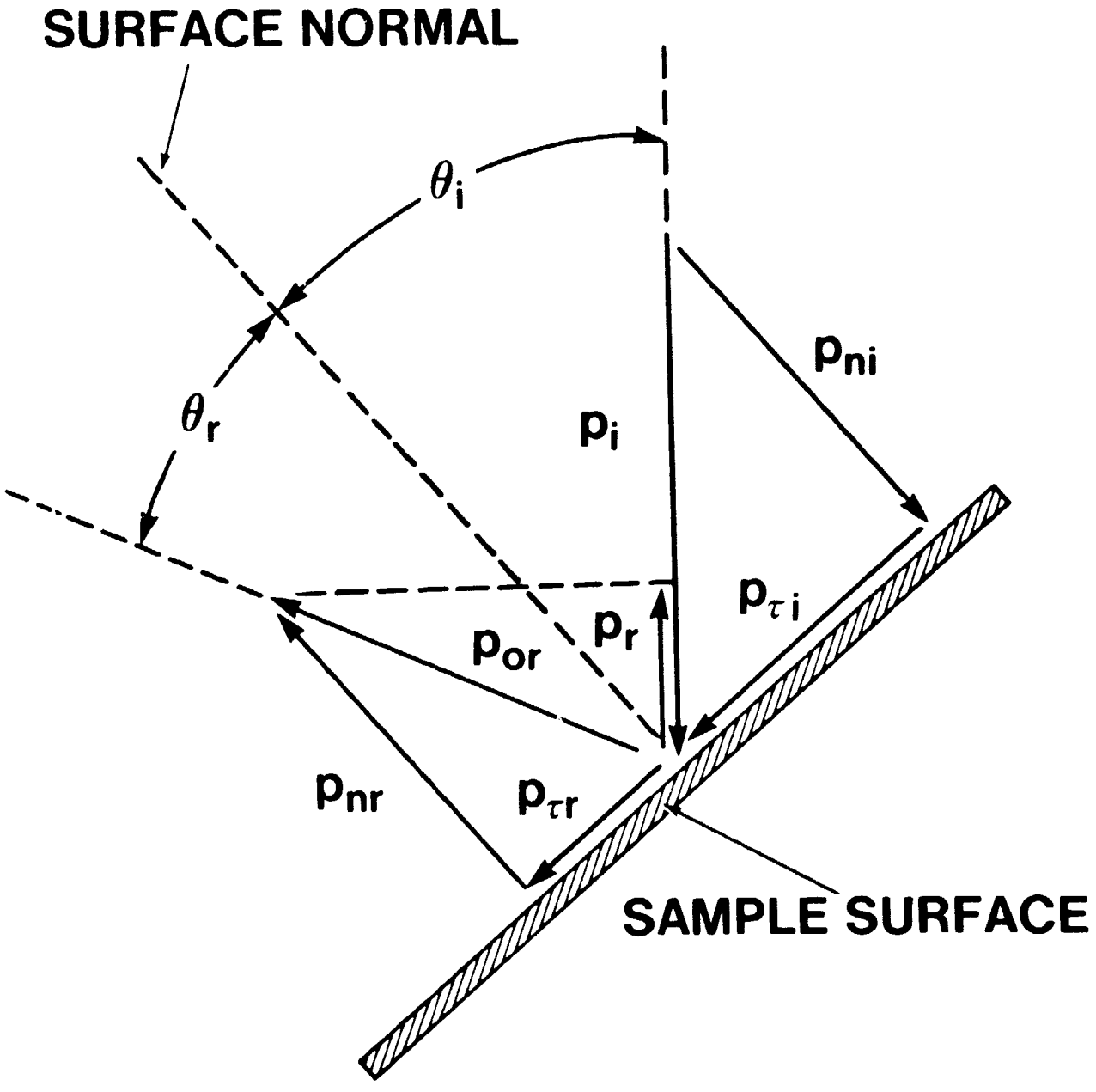

Figure 6. Definition of momentum vectors used in the text. Note that p_r is the component of the total reflected momentum (shown by p_{or}) along the line of p_i.

The measurements of Knechtel and Pitts were reduced by them to the standard definition of equations (7) and (8). However, they did not specify the surface temperature for their experiments, and thus there is an uncertainty in the value of p_s that should go into eq (7). We use the relation given by them to obtain p_s. Assuming a surface temperature T_s equal to room temperature, 300°K, we get

$$p_s \simeq \frac{0.038\ p_i}{\cos \theta_i} \quad . \tag{37}$$

We substitute eq (37) into (7) and get

$$\alpha_n = \frac{p_{ni} - p_{nr}}{p_{ni}\,(1 - 0.038/\cos^2\theta_i)} \quad . \tag{38}$$

Using eq (38) in place of eq (34) we rederive the equation for p_r/p_i:

$$\frac{p_r}{p_i} = (1 - \alpha_n)\cos^2\theta_i - (1 - \alpha_\tau)\sin^2\theta_i + 0.038\ \alpha_n \quad . \tag{39}$$

The accommodation coefficients of Knechtel and Pitts are given in columns 5 and 6, and the p_r/p_i ratios deduced from them with eq (39) are given in column 7. The difference between eqs (39) and (36) is just the term $0.038\ \alpha_n$. The coefficient 0.038 was obtained using the temperature T_s of 300°K above. The coefficient is proportional to $\sqrt{T_s}$, so unless T_s was extremely high, the uncertainty should remain small.

We have plotted the ratio $f(\theta) = p_r/p_i$ for the three experiments in Figure 7. Before comparing these results, we must review briefly the differences between the measurements. The data of Seidl and Steinheil (SS) was obtained from the impact of a beam of He atoms on a sapphire surface. Their beam energy of 0.05 eV corresponds to a velocity of roughly 2 km/s. The data of Knechtel and Pitts (KP) corresponds to the impact of N_2 or N_2^+ on Aluminum surfaces at an

Table 1. Measured α_n, α_τ and p_r/p_i vs. angle of incidence θ_i

θ (deg)	α_n^a	α_τ^a	$(p_r/p_i)^a$	α_n^b	α_τ^b	$(p_r/p_i)^b$	$(p_r/p_i)^c$
0	0.74		0.26	0.91		0.13	0.17 ± .02
10	0.75 ± .03	0.74 ± .12	0.23				
20	0.73	0.73	0.21				
30	0.70	0.72	0.16	0.85	0.42	0.00	
40	0.62 ± .06	0.72	0.11				
45				0.76	0.54	- 0.08	0.07 ± .03
50	0.52	0.72	0.04				
60	0.38	0.72	- 0.06	0.60	0.51	- 0.25	- 0.02 ± .01
70	0.16 ± .10	0.70 ± .03	- 0.17				
75							- 0.23 ± .05

(a) Seidl and Steinheil (1974)

(b) Knechtel and Pitts (1973)

(c) Boring and Humphris (1973)

energy of 10 eV which gives a velocity roughly equal to 8 km/s. The data of Boring and Humphris (BH) represents N_2, N_2^+, and O or O^+ impact on test surfaces from satellite Echo 1 and Explorer XXIV. The kinetic energy of 5 eV of the O^+ beam also corresponds to an 8 km/s velocity. In general, measurements indicate that p_r p_i should decrease as the velocity increases, and the difference between SS (circles) and KP (x's) is consistent with this fact. The BH (squares) values are markedly higher than the KP values. Additional measurements have been made, but have not been included here because of the preliminary status of this part of the report.

We note that the KP values, extrapolated to $\theta = 84°$ (see discussion regarding eq (19)), give $f(\theta) \simeq -0.6$ in Figure 7. This gives a lateral surface coefficient $C_{1S} \simeq 0.04$ using eq (33). On the other the BH data extrapolate to roughly $f(\theta) = -0.4$ at $\theta = 84°$. This gives $C_{1S} \sim 0.06$ in agreement with the value obtained in section IV from the flight data. This agreement is probably fortuitous. We point out that the angle $\bar{\theta}_i = 84°$ may be in error by perhaps + 3°, and careful computation including the angular distribution of gas molecules incident on the surface is required before a better value of $\bar{\theta}_i$ is known. However, it is clear that predictions of drag using the data of Boring and Humphris will be higher than with the data of Knechtel and Pitts.

We noted in the introduction that previous extrapolations of the data Knechtel and Pitts appeared to overestimate the drag coefficient. The extrapolation was presented by Fredo and Kaplan (1981), and they obtained $\alpha_\tau \simeq 0.6$ and $\alpha_n \simeq 0.25$ at $\theta = 90°$. Substituting these values into eq (39), we get $f(90°) \simeq -0.3$. In our computation, the corresponding value $f(84°)$ would be about -0.25, and would give $C_{1S} \simeq 0.08$. This is roughly 30% larger than the value of 0.06 obtained above, and about twice as high as the value $C_{1S} \simeq 0.04$, obtained with the interpolation done here.

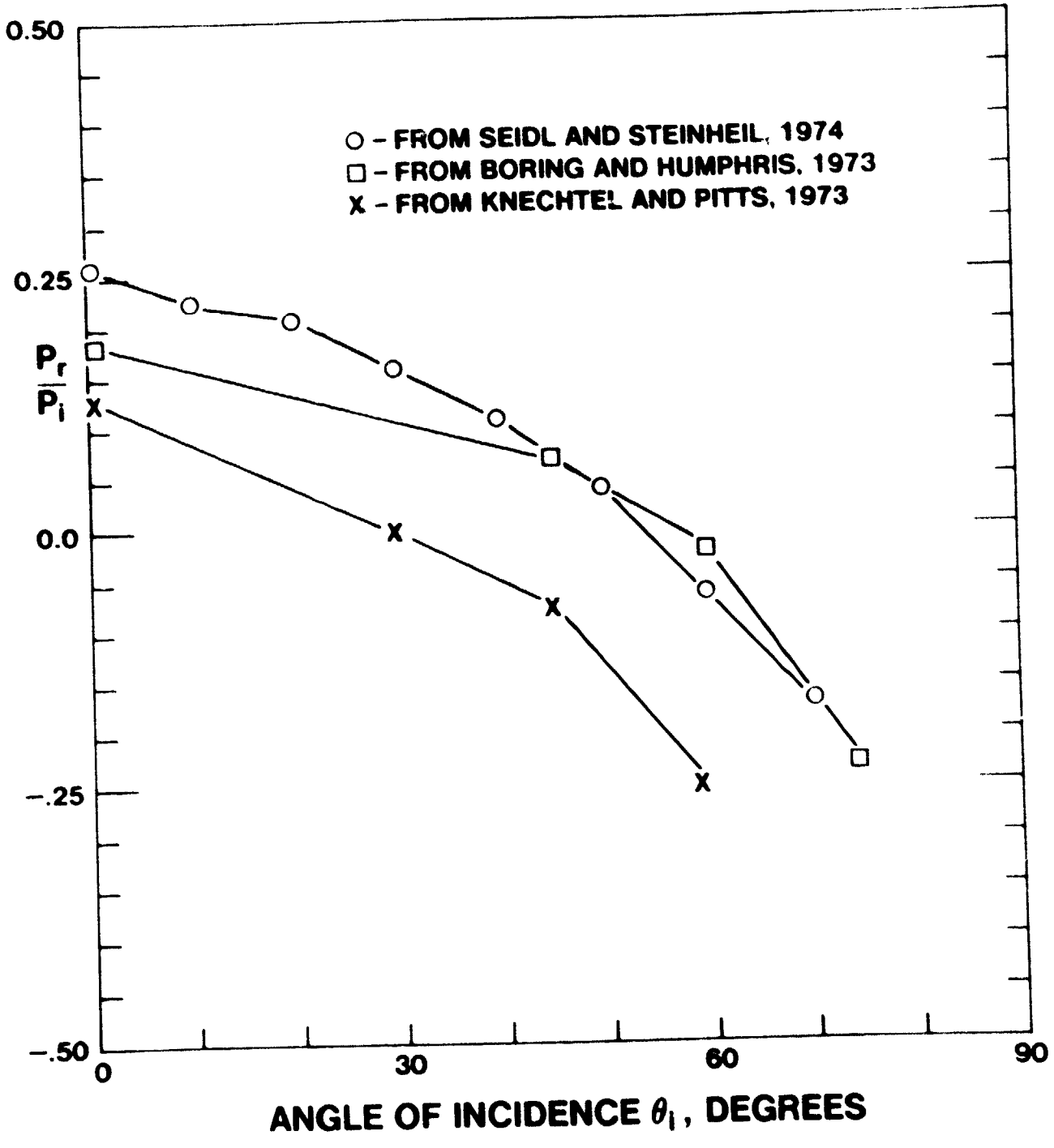

Figure 7. Comparison of the ratio P_r/P_i obtained from the three experiments referenced. The values plotted are given in Table I.

VI. CONCLUSIONS

1. We have derived an equation which allowed us to obtain the drag coefficient for the bare GRM cylinder independently of laboratory measurements, and found that the value obtained leads to a ratio p_r/p_i which is consistent with the published laboratory estimates. This degree of consistency lends confidence to our estimate. Using flight data for a spacecraft with an L/r ratio of 15, we obtained upper and lower bounds for the lateral surface coefficient C_{LS} of eq (32). With those values of C_{LS}, we obtained upper and lower bounds of 2.9 and 2.7 for the bare GRM cylinder with L/r = 10. The coefficient C_{LS} indicates a value of $p_r/p_i \simeq -0.4$ at angles of incidence near 84°. These values of p_r/p_i are reasonable extrapolations of the laboratory results.

2. It is implicit in the conclusion above and in eq (32) that the contribution to the drag from the sides of the cylinder decreases as the angle θ approaches 90°. It should prove useful to compute the average angle $\bar{\theta}_i$ of eq (19) when the lateral surface normal has a small component in the direction opposite the direction of flight. Such a situation would occur if our cylinder was deformed by reducing the diameter of the back plate slightly. The cylinder then becomes a frustrated cone of small half-angle flying with its base forward. The number of molecules impacting the sides decreases with the half-angle of this cone, and significant reduction in drag should result. Computations are in progress to estimate the reduction in C_{LS} with the conical deformation of the cylinder proposed here.

3. The solar panels and other smaller appendages on the GRM will contirbute to make the actual drag coefficient larger than that obtained for the bare cylinder. The computation of C_{LS} and the work in progress mentioned above should provide the basis for an estimate of this effect in the immediate future.

4. The comparison of laboratory data suggests that a more careful extrapolation of the measurements of Knechtel and Pitts (1973) may give lower drag coefficients using the method

outlined by Schaaf and Chambre (1958), and used by Fredo and Kaplan (1981) and Ray and Jenkins (1981).

5. Finally, every effort should be continued to acquire more information on drag coefficient determinations for other cylindrical spacecraft such as the SETA-1 and SETA-2 in order to lend more confidence yet to our estimates, and with a view to estimate the effect of solar panels and the efficiency of shadowing of one surface by another.

REFERENCES

Boring, J. W., and R. R. Humphris, Drag Coefficients for Spheres in Free Molecule Flow in O at Satellite Velocities, NASA report no. CR-2255, March 1973.

Cook, G. E., Satellite Drag Coefficients, Planet. Space Sci., 13, 929-946, 1965.

Devienne, F. M., J. Souquet and J. C. Roustan, Study of the Scattering of High Energy Molecules by Various Surfaces in Rarefied Gas Dynamics, Vol. 2, Suppl. 3, pp. 584-594, ed. J. H. de Leeuw, Academic Press, New York, 1966.

Fredo, R. M. and M. H. Kaplan, Procedure for obtaining aerodynamic properties of spacecraft, J. Spacecraft, 18, 367-373, 1981.

Jakus, K., and F. C. Hurlbut, Gas Surface Scattering Studies Using Nozzle Beams and Time-of-Flight Techniques, in Rarefied Gas Dynamics, Vol. 2, Suppl. 5, pp. 1171-1185, ed. L. Trilling and H. Y. Wachman, Academic Press, New York, 1969.

Knechtel, E. D., and W. C. Pitts, Normal and Tangential Momentum Accommodation for Earth Satellite Conditions, Astronautica Acta, 18, 171-184, 1973.

Loeb, L., The Kinetic Theory of Gases, pp. 278-348, Dover Publications, New York, 1961.

Moe, M. M., and L. C. Tsang, Drag coefficients for cones and cylinders according to Schamberg's model, AIAA Journal, 11, 396-399, 1973.

O'Keefe, D. K. and J. B. French, High Energy Scattering of Inert Gases from Well Characterized Surfaces I. Experimental, in Rarefied Gas Dynamics, Vol. 2, Suppl. 5, p. 1279-1296, ed. L. Trilling and H. Y. Wachman, Academic Press, New York, 1969.

Ray, J. C., and R. E. Jenkins, GRAVSAT/MAGSAT-A Guidance and Control System Annual Report 1981, Volume I, JHU/APL SDO 6179, The Johns Hopkins University, Applied Physics Laboratory, Columbia, Maryland, 1981.

Robertson, A., Comparison of Flight-measured Drag Characteristics with Pre-flight Predictions, Internal Report 71-5131.1-34, The Aerospace Corporation, El Segundo, California, July 1971.

Schaaf, S. A., and P. L. Chambre, Flow of Rarefied Gases, in Fundamentals of Gas Dynamics, ed. H. W. Emmons, Princeton University Press, Princeton, N.J., 1958.

Seidl, M., and E. Steinheil, Measurement of momentum accommodation coefficients on surfaces characterized by Auger Spectroscopy, SIMS and LEED, in Rarefied Gas Dynamics, Proceedings of 9th International Symposium 1974, vol. II, pp. E.9-1 to E.9-12, ed. M. Becker and M. Fiebig, DFVLR-Press, Porz-Wahn, Germany, 1974.

Spencer, N. W., H. B. Niemann, and G. R. Carignan, The neutral atmosphere temperature instrument, Radio Sci., 8, 284, 1973.

Smith, J. N., Jr., and H. Saltsburg, Recent Studies of Molecular Beam Scattering from Continuously Deposited Gold Films, in Rarefied Gas Dynamics, Vol. 2, Suppl. 3, pp. 491-504, ed. J. H. de Leeuw, Academic Press, New York, 1966.

Thomas, L. B., Accommodation of Molecules on Controlled Surfaces, Rarefied Gas Dynamics, vol. 74, part I, pp. 83-108, AIAA, New York, 1980.

Tsien, H. S., Superaerodynamics, Mechanics of Rarefied Gases, J. Aeronaut. Sci., 13, 653-664, 1946.

U. S. Standard Atmosphere, 1976, U. S. Government Printing Office, Washington, D.C., 1976.

END

DATE

FILMED

SEP 13 1983